

PAPER • OPEN ACCESS

Raman imaging to study structural and chemical features of the dentin enamel junction

To cite this article: M Anwar Alebrahim *et al* 2015 *IOP Conf. Ser.: Mater. Sci. Eng.* **92** 012014

View the [article online](#) for updates and enhancements.

You may also like

- [Femtosecond laser ablation of dentin](#)
S Alves, V Oliveira and R Vilar

- [Low- and high-density InAs nanowires on Si\(0 0 1\) and their Raman imaging](#)
Suparna Pal, S D Singh, V K Dixit *et al.*

- [Advanced imaging of dentin microstructure](#)
T A Bakhsh, J A Abuljadayel, E Alshouibi *et al.*



ECS Membership = Connection

ECS membership connects you to the electrochemical community:

- Facilitate your research and discovery through ECS meetings which convene scientists from around the world;
- Access professional support through your lifetime career;
- Open up mentorship opportunities across the stages of your career;
- Build relationships that nurture partnership, teamwork—and success!

Join ECS!

Visit electrochem.org/join



Raman imaging to study structural and chemical features of the dentin enamel junction

M. Anwar Alebrahim^{1,2}, C. Krafft¹, and J. Popp^{1,3}

¹ Leibniz Institute of Photonic Technology, Jena, Germany

² Jordan University of Science and Technology, Irbid, Jordan

³ Institute of Physical Chemistry and Abbe Center of Photonics, University Jena, Jena, Germany.

E-mail: marnah@yahoo.com

Abstract. The structure and chemical features of the human dentin enamel junction (DEJ) were characterized using Raman spectroscopic imaging. Slices were prepared from 10 German, and 10 Turkish teeth. Raman images were collected at 785 nm excitation and the average Raman spectra were calculated for analysis. Univariate and multivariate spectral analysis were applied for investigation. Raman images were obtained based on the intensity ratios of CH at 1450 cm⁻¹ (matrix) to phosphate at 960 cm⁻¹ (mineral), and carbonate to phosphate (1070/960) ratios. Different algorithms (HCA, K-means cluster and VCA) also used to study the DEJ. The obtained results showed that the width of DEJ is about 5 μm related to univariate method while it varies from 6 to 12 μm based on multivariate spectral technique. Both spectral analyses showed increasing in carbonate content inside the DEJ compared to the dentin, and the amide I (collagen) peak in dentin spectra is higher than DEJ spectra peak.

1. Introduction

Enamel, dentin and cementum are the major tissues which make up the tooth in humans. Enamel is the hardest and most highly mineralized substance in the human body with a mineral content of 96%. The mineral content of dentin is reduced to approximately 70% whereas the organic content is increased to 20%. Enamel's and dentin's most abundant mineral is hydroxyapatite, which is a crystalline calcium phosphate. The dentin-enamel junction, abbreviated DEJ, is the interface between the enamel and the underlying dentin. DEJ is known for its unique biomechanical properties that provide a crack-arrest barrier for flaws formed in the brittle enamel [1]. The DEJ structure is generally described as a series of 25–100 μm diameter scallops with their convexities directed toward the dentin [2, 3]. The DEJ is also investigated by parallel 80–120 nm diameter collagen fibrils that directly insert into the enamel mineral and also merge with the interwoven fibrillar network of the dentin collagen matrix [4]. It is thought that the DEJ is greatly influenced by enamel knots that form before the



mineralization of the tissue secret [5]. Lucas (2004) describes that the first enamel formed, at the DEJ, has not been well studied, and appears to have a random orientation under light microscope [6]. The structure and chemical composition of the human dentin-enamel junction (DEJ) was studied using confocal Raman microscopy and the authors reported that the Phosphate to organic ratio showed an accumulation of organic material under the enamel surface and high phosphate content compared to enamel in the vicinity of the DEJ [7]. During recent years, vibrational spectroscopic imaging has matured into an important tool for the study of musculoskeletal tissues. Both IR and Raman spectroscopies contain signatures for the stages of development, for tissue disease and damage, and even for mechanical properties. Raman spectroscopy is non-destructive and label-free vibrational spectroscopic technique that enables structural and chemical analysis of mineralized tissue such as bone and teeth. Two dimensional Raman mapping/imaging of the specimen enables us to obtain spectra at points on the specimen separated by 1 μm . Thus the data consists of three dimensions – the x and y coordinates at every pixel and the intensity value at each Raman shift of the spectrum at that pixel. The data thus obtained is known as hyperspectral data, in view of its large size in each dimension. Therefore, analysis of the hyperspectral data is very important to give a spatial distribution of the chemical makeup of the specimen. However, analysts apply different techniques such as univariate and multivariate analysis for well understand the data. Univariate methods consider one wave number, of the Raman shift, presenting results about only characteristic functional group based on a particular wave number not on all pixels as a whole. Multivariate analysis methods help to analyze the hyperspectral data by manipulating each spectrum as a whole, rather than corresponding individual peaks in each spectrum [8].

The aim of this computing was to apply univariate and multivariate analysis to characterize the structural and chemical properties of dentin enamel junction by using Raman imaging.

2. Materials and methods

2.1. Specimen preparation

Six primary and four permanent non-carious, human teeth were provided from the Department of Conservative Dentistry, University Hospital Jena, Germany. Six primary and four permanent non-carious, human teeth were collected under informal consent from children and adults in Hacettepe University, Ankara, Turkey. Soft tissue remnants of contemporary samples were quickly removed from the root surface. The samples were stored in an aqueous solution of 4% formalin to inhibit the microbial growth. German specimens were embedded in Kallocryl-CPGH red and Turkish specimens in autopolymerizing polymethylmethacrylate (PMMA). A stainless steel saw with galvanic diamond coating, grain size 120 micron and 4 cm diameter (Komet, Germany), was used to prepare 1–2 mm thick slices. The specimens were manually polished before the measurements were performed.

2.2. Raman spectroscopic imaging

A single mode diode laser (model Xtra, Toptica, Germany) with 785 nm emission was coupled to a microscope and the microscope was coupled to the Raman spectrometer (RXN1 microprobe, Kaiser Optical System, USA). The laser light with an intensity of 100 mW was focused on the sample with a 100x/NA 0.9 objective (Nikon, Japan). The Raman signal was detected on a Peltier-cooled (-60°C), back-illuminated, deep-depletion CCD chip (Andor, Ireland). Images were obtained over the spectral region of 200 to 3450 cm^{-1} at spectral resolution of 4 cm^{-1} with a step size of 1 μm and 6 s exposure time plus 3 s dwell time per Raman spectrum. The Holograms software (Kaiser) automatically performed corrections of dark counts, cosmic spikes, and calibrations of the wavenumber and intensity axis.

3. Result and discussion

Figure1A represents the tooth slice illustrating where spectral maps were obtained. Regions of interest were selected from normal appearing sites. Figure1B shows Raman spectra (800 - 1800 cm^{-1}) of

human dentin and enamel. The difference spectrum of dentin minus enamel was calculated to better visualize the organic bands. The bands associated with inorganic component (mineral) appeared in the spectral range from 900 to 1100 cm^{-1} , including ν_1 and ν_3 vibration bands. The organic components (collagen) appeared in the spectral region of 1200 to 1720 cm^{-1} . Moreover, the most intense peak on Raman spectra is the symmetric stretch vibration of PO_4^{2-} at 962 cm^{-1} . The Raman assignments are included in table 1.

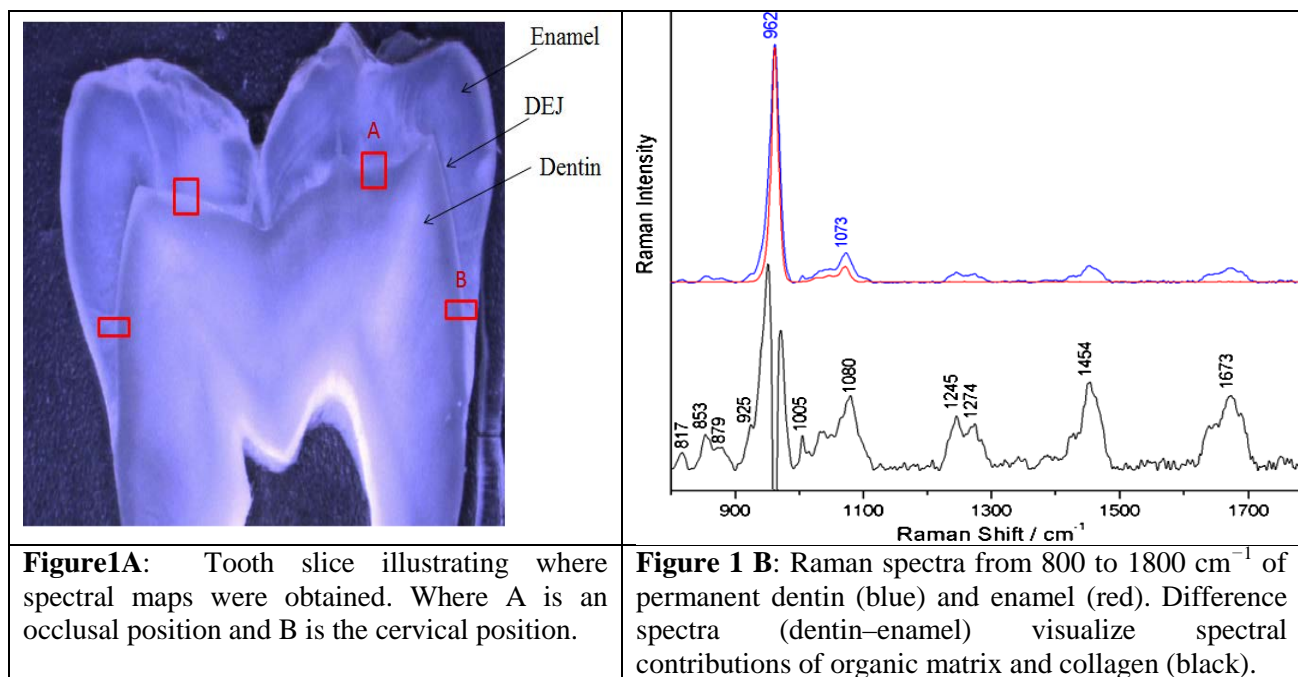


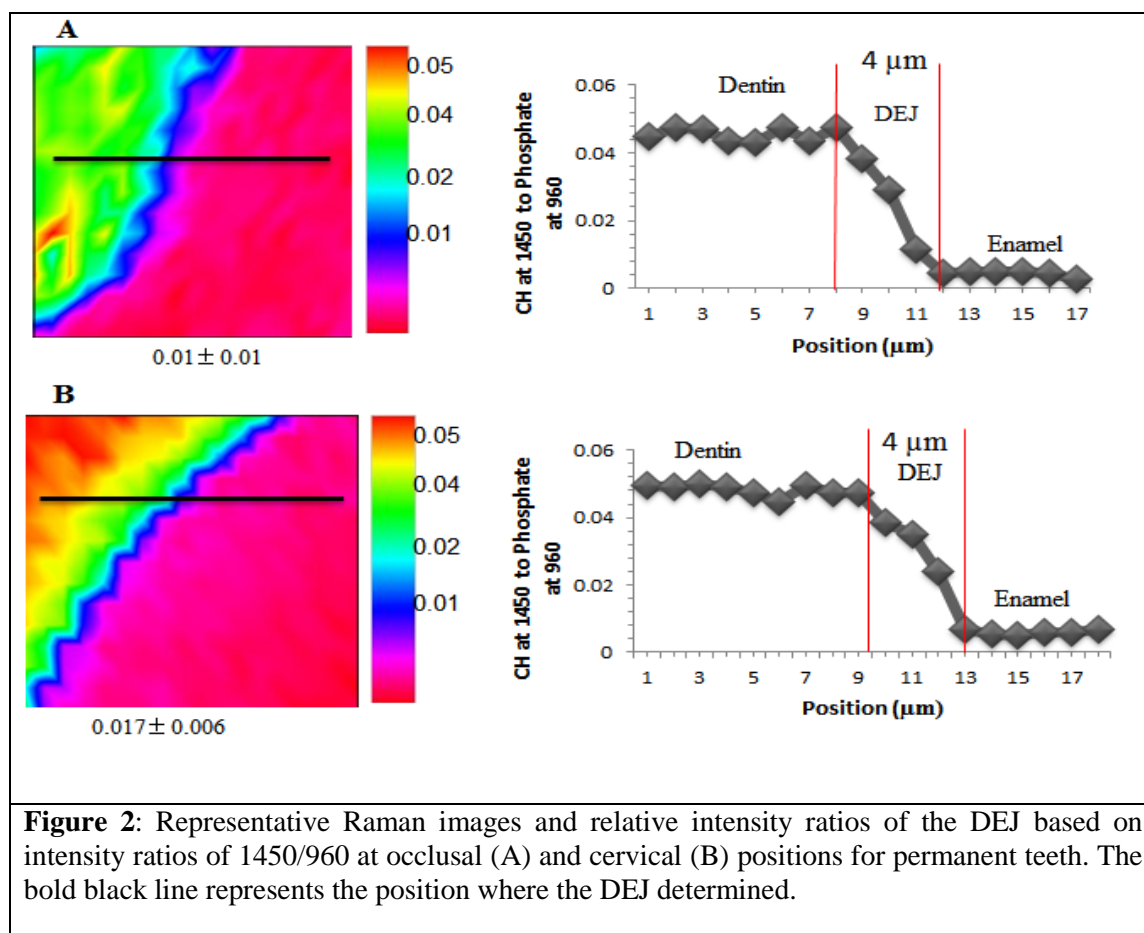
Table 1: Band assignment in Raman spectra of enamel and dentin [9]

Raman band	Assignment
817, 853, 920	Collagen
960	ν_1 of PO_4^{3-}
1005	Collagen (Phe)
1070	ν_1 of CO_3^{2-}
1248, 1273	Collagen (amide III)
1450	Collagen (CH_2)
1670	Collagen (amide I)

3.1. Univariate spectral analysis

Representative Raman mapping results of the DEJ at occlusal and cervical sites of a human tooth are shown in figure 2 A and B, respectively. Raman images were obtained based on the intensity ratios of CH at 1450 cm^{-1} (matrix) to phosphate at 960 cm^{-1} (mineral). The relative matrix/mineral (1450/960) ratios are represented by the color differences. Red/pink color represents the lower relative ratio (Enamel), while green/yellow/orange represents the higher relative ratio (dentin). A region where the color changes from blue is related to the DEJ transition zone. Comparison of the two images indicates that the width of DEJ transition zone at cervical position is the same of at occlusal position, and it equals to 4 μm based on the univariate method spectral analysis.

The representative relationships of the carbonate to phosphate (1070/960) ratios as a function of positions across the DEJ transition zone are shown in figure 3A and B. The matrix/mineral ratios of the DEJ were higher than those of enamel and lower than those of dentin. These ratios of the DEJ gradually increased during the transition from the enamel to dentin zone. The width of transition zone equals to 5 μm at both positions (occlusal & cervical). On the other hand, average Raman spectra from the dentin and DEJ area in the protein- derived spectral region of 1200- 1750 cm^{-1} are shown in figure 4A, in which the vibration peak of CH at 1450 cm^{-1} was selected as internal standard for the normalization adjustment. As compared to dentin spectra, the amide I (collagen) peak increased, but the amide III peak decreased in the DEJ spectra. Also the average spectra from the dentin and DEJ zone in the spectral region of 900- 1200 cm^{-1} are shown in figure 4B. The spectra were normalized based on phosphate peak at 960 cm^{-1} . The spectra showed that the peak at 1070 cm^{-1} which is related to the carbonate type-B from the DEJ spectra is higher than the carbonate peak from the dentin average spectra.



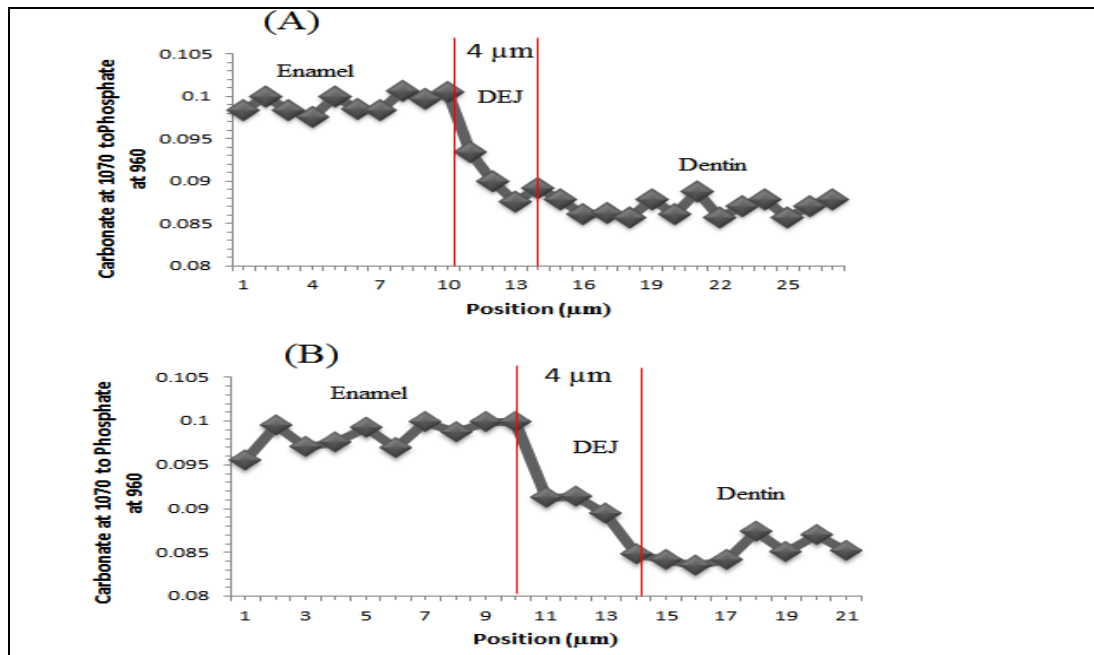


Figure 3: relative intensity ratios of 1070/960 across the enamel/DEJ/dentin zone at occlusal (A) positions and at cervical (B) positions.

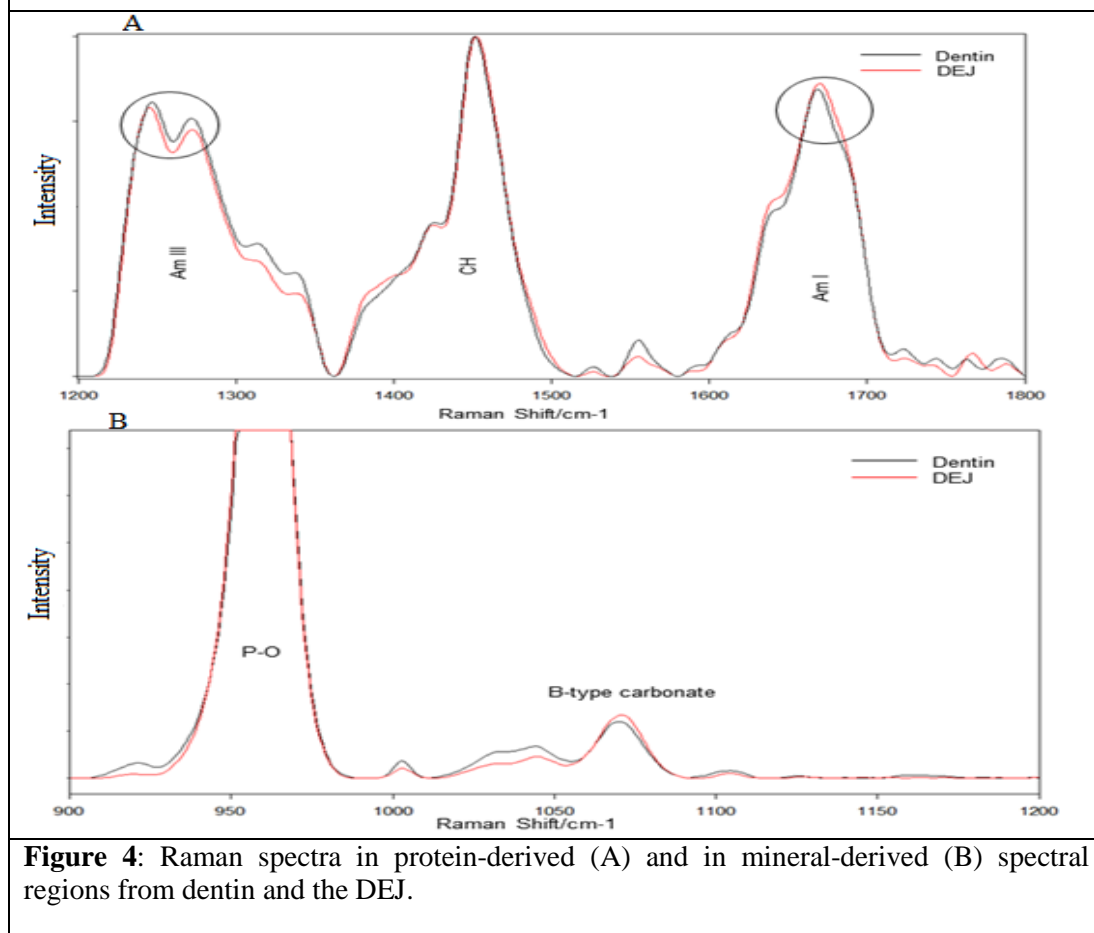


Figure 4: Raman spectra in protein-derived (A) and in mineral-derived (B) spectral regions from dentin and the DEJ.

3.2. *Multivariate spectral analysis*

Raman spectra collected are often contaminated with various interfering signals. The sources of interference include fluorescence and stretching of spectral intensity amplitudes [8]. The amplitude stretching (intensity variations) could be due to specimen inclination, variation in specimen thickness and absolute intensity of light. For instance, mineral and protein contents of dentin show variations compared to the enamel. In order to eliminate interfering signals and bring the spectra to a common platform of comparison, some preprocessing were performed. Data was carried out by using the Cytospec software and MatLab procedures written in-lab. A baseline correction by polynomial fitting of a second degree was used to remove of the florescence background with no smoothing.

3.2.1. *K-Means Cluster & hierarchical cluster analysis result*

Cluster analysis is an unsupervised statistical method of grouping the data, without a priori knowledge of its nature. The initial centroids of K-means clustering are randomly chosen. The distances are calculated between a spectrum and the centroid. Then each spectrum is assigned to the cluster whose centroid is nearest and the data set is grouped into a preselected number (K) of clusters. Figure 5 A, B, C & D shows the HCA & k-means cluster analysis maps of 70 μm X 70 μm of Raman image A& B and Raman averaged spectra of protein and mineral region C & D. HCA and K-means cluster analysis showed identical result to distinguish the transition zone of DEJ across the enamel and dentin. The cluster analyses do not give a fixed width for the DEJ. The width was varied from 6 μm in narrower width to the wider width of 12 μm . In HCA we were used three clusters (enamel, DEJ, and dentin). While in K-means analysis, five clusters were used (figure 5 B). The first two clusters were related to the enamel and DEJ and the rest were attributed to dentin region. Dentin contains around 75% in mineral (HAP) and 25% proteins and water. On the hand the enamel contains 99% in mineral considering a homogeneous layer. Based on that different content the K-means cluster analysis carried out by using more than three clusters to give agreement result with the HCA cluster analysis. On the other hand the molecular features of DEJ in comparison to the dentin and enamel were the same results from HCA and K-means cluster analysis. In protein spectral Raman region (figure 5 C) after normalization based on CH band, the amide I and amide III peaks in dentin were higher than DEJ spectra peaks. The mineral Raman spectral region (figure 5 D) normalized to phosphate peak at 960 cm^{-1} . Moreover the intensity of carbonate at 1070 cm^{-1} increased from dentin to enamel across the DEJ area indicating the lower carbonate contents in dentin.

3.2.2. *Vertex component analysis (VCA)*

VCA offers an unsupervised solution to the blind source separation problem. VCA represents the image raw data in a space of smaller dimensionality aiming to retain all relevant information and it calculates endmembers instead of loadings. Scope of VCA is that endmembers represent spectra of most dissimilar chemical constituents. Then, scores denote the concentration of the endmember spectra. The VCA algorithm iteratively projects data onto a direction orthogonal to the subspace spanned by the endmembers already determined. Figure 6 shows the Raman image of vertex component analysis, the composite image, dentin in red, DEJ in blue and the enamel in green (A) and three components with its related spectra (B). It showed that the DEJ width varies from 12 microns in some positions to 6 microns on another positions. On the hand, the organic components in DEJ were not clearly observable compared to the dentin, while the mineral in DEJ clearly appeared to be higher than dentin in comparison to the intensity of the phosphate band at 960 cm^{-1} as shown in figure 6 B. Usually the interface between two materials with different mechanical properties like elasticity is a weak link in structure. The DEJ zone acts to transfer applied loads from the enamel to dentin like during the masticatory or impact and also to inhibit the crack propagation. However, many different instruments have been used to identify the DEJ, such as SEM, Raman spectroscopy and optical spectroscopy. The researchers were reported different width to the transition area, for example it was

reported that the DEJ width varies from 50 to 100 μm [4], 10 μm [10] and around 2-3 μm [11]. DEJ width has been investigated later to be dependent on the intratooth location and the authors reported that the mean width is $12.9 \pm 3.2 \mu\text{m}$ at occlusal position and $6.3 \pm 1.3 \mu\text{m}$ at cervical position. To date, there has been minimal chemical information related to the DEJ transition zone due to its small size [12]. In this study, it is the first time that we used the multivariate analysis in detection of transition zone. The obtained results from different algorithms (HCA, K-means cluster and VCA) were indicated that the width of transition zone varies as a function of position in microscale. However, the chemical structure features based on multivariate analysis suggested that the amide I and amide III peaks decreased in DEJ in comparison to the dentin Raman peaks. The decrease in these peaks could be related to the increasing disorder of the functional groups in organic matrix [13]. The spectral differences indicate that the structure of organic matrix in the dentin and DEJ was diverse. Formation of the DEJ begins at the early stages of tooth morphogenesis and is thought to be linked to a mixture of dentin proteins secreted by odontoblasts and enamel proteins from ameloblasts [13-15]. The proteins associated with DEJ formation and collagen fibril bundles that cross the transition zone and insert into enamel [4] might be responsible for the variations and distribution deviations in composition and structure of the organic matrix within the DEJ. The width and shape of phosphate peak at 960 cm^{-1} of dentin and DEJ spectra were similar and no significant change. This indicating that the mineral crystallinity within the DEJ might be not much different compared to the mineral of dentin, (figure 6.B).

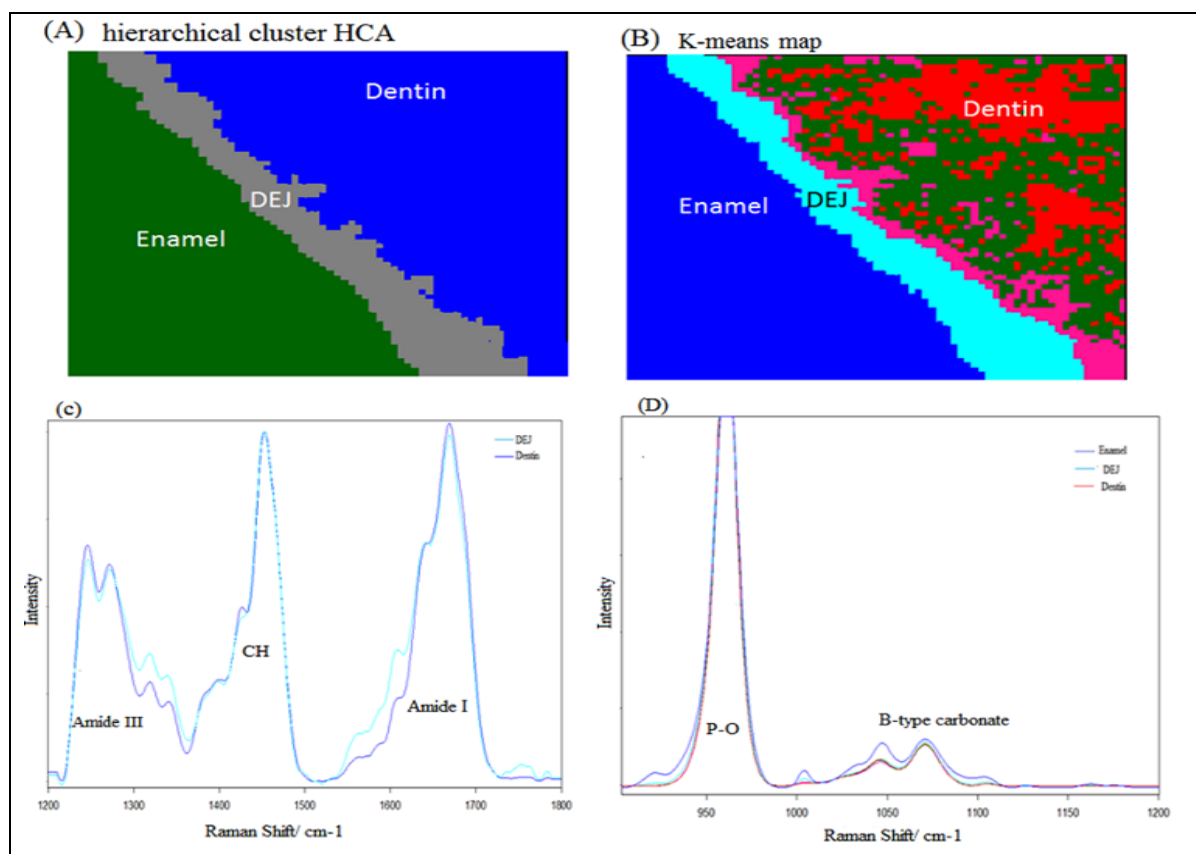


Figure 5: Map of hierarchical cluster analysis (A) and map of k-means cluster analysis (B) of a $70 \times 70 \mu\text{m}$ Raman image from permanent human teeth. The cluster averaged Raman spectra derived from k-means cluster analysis of protein region from 1200 to 1800 cm^{-1} (C) and the Raman averaged spectra of mineral region constructed from k-means analysis of mineral spectral region of $900 - 1200 \text{ cm}^{-1}$ (D).

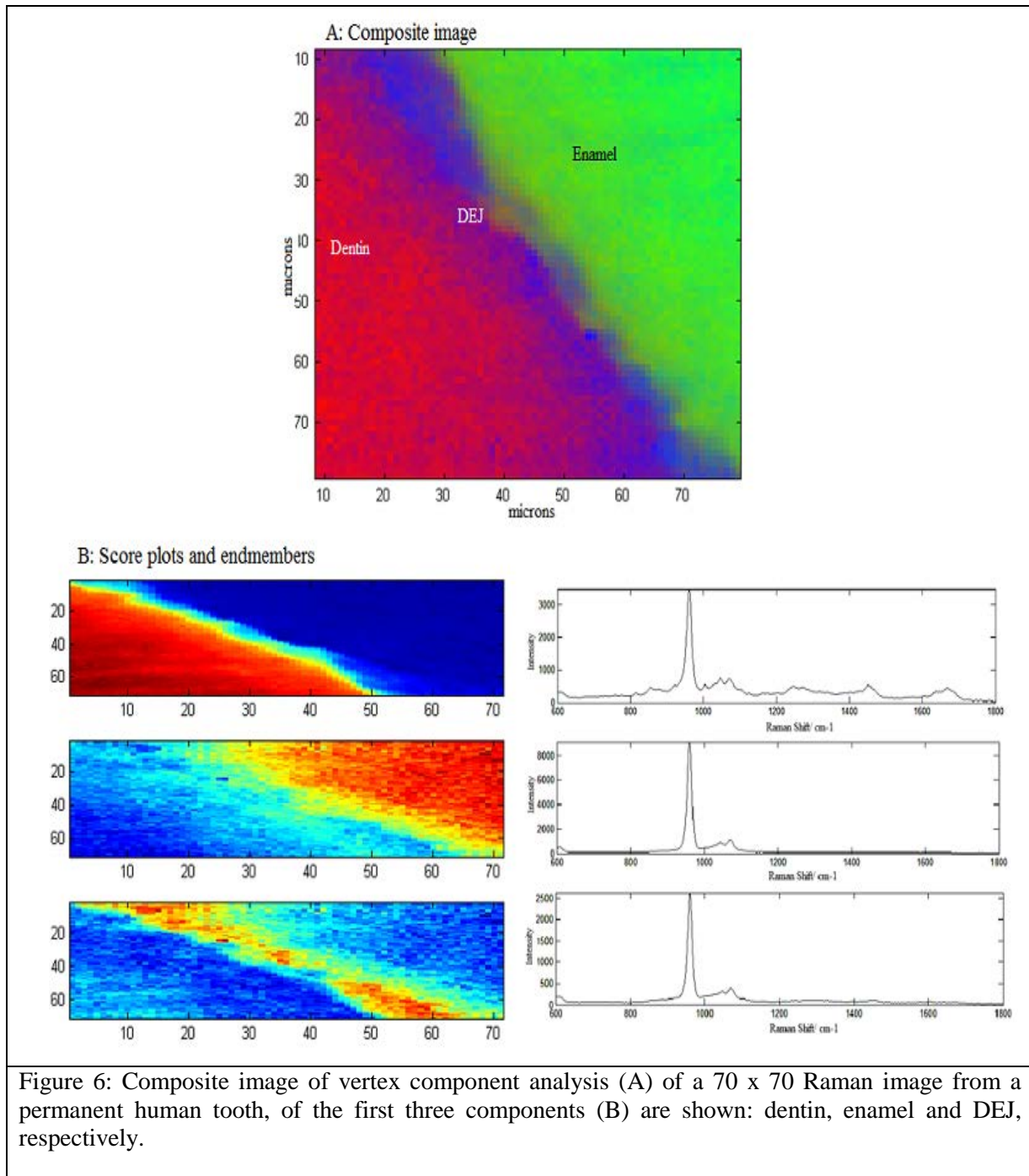


Figure 6: Composite image of vertex component analysis (A) of a 70 x 70 Raman image from a permanent human tooth, of the first three components (B) are shown: dentin, enamel and DEJ, respectively.

4) Conclusion

Limited work has been done to study the DEJ by Raman imaging, the data were analyzed by applying univariate and multivariate methods analysis. Univariate spectral analysis might be not suitable spectral technique to characterize the DEJ, especially for the DEJ width which was not more than 5 μm in comparison to the multivariate spectral analysis. . The obtained results from different algorithms (HCA, K-means cluster and VCA) confirm each other, were indicated that the width of

transition zone (DEJ) varies as a function of position in microscale. The molecular features derived from univariate and multivariate spectral analysis showed increasing in carbonate content inside the DEJ compared to the dentin. VCA showed similarity of the width and shape of phosphate peak at 960 cm^{-1} of dentin and DEJ spectra, indicating the mineral crystallinity within the DEJ is not much different compared of the mineral crystallinity of dentin. Both methods showed that the amide I peak in dentin was higher than DEJ spectra peak. These results probably give more information beside the published scientific articles in the literature for understanding of this critical zone.

References

- [1] Imbeni V, Kruzic J J, Marshall G W, Marshall S J, and Ritchie R O 2005. *Nature materials* **4**, 229 - 232
- [2] Avery J K, Steele P F, editors 2002 Oral Development and History. New York p. 74
- [3] Ten Gate, AR. 1994 Oral Histology. Mosby; St Louis
- [4] Lin C P, Douglas W H, Erlandsen S L 1993. *Journal of Histochemistry and Cytochemistry* **41**:381. [PubMed: 8429200]
- [5] Tafforeau P and Smith T M *Journal of Human Evolution*. **54**, P. 272- 278
- [6] Lucase P W 2004. *Cambridge University Press*, Cambridge, UK
- [7] Desoutter A, Salehi H, Slimani A, Marquet P, Jacquot B, Tassery H, Cuisinier F J G 2014 *Lasers in Dentistry* SPIE 8929
- [8] Ranganathan Parthasarathy, Ganesh Thiagarajan¹, Xiaomei Yao, Yu-Ping Wang, Paulette Spencer, and Yong Wang 2008. *J.Biomed Opt* **13** (1)
- [9] M. Anwar Alebrahim, C. krafft, W. Sechaneh, B. Sibusch, and J. Popp 2014. *Biomedical Spectroscopy and Imaging*. **3** P. 15-27
- [10] Marshall Jr G W, Balooch M, Gallagher R R, Gansky S A, Marshall S J 2001. *J. biomed Mater Res* **54**, P. 87–95.
- [11] Balooch G, Marshall G W, Marshall S J, Warren O L, Asif S A S, Balooch M 2004. *J Biomech*. **37** P. 1223-32
- [12] Xu C, Yao X, Walker M P, and Wang Y 2009. *Calcif Tissue Int*. **84** (3) P. 221- 228
- [13] Nagano J T, Oida S, Ando H, Gomi K, Arai T, and Fukae M 2003 *J Dent Res*. **82**, P.982–986.
- [14] Begue-Kir C, Krebsbach P H, Bartlett J D, Butler W T 1998 *Eur J Oral Sci*. **106**, P. 963–970.
- [15] Nanci A, Zalzal S, Lavoie P, Kunikata M, Chen W, Krebsbach P H, et al 1998 *J Histochem Cytochem*. **46**, P.911–934.